



Competition between stationary and oscillatory viscoelastic thermocapillary convection of a film coating a thick wall



I.J. Hernández Hernández, L.A. Dávalos-Orozco*

Instituto de Investigaciones en Materiales, Departamento de Polímeros, Universidad Nacional Autónoma de México, Ciudad Universitaria, Circuito Exterior S/N, Delegación Coyoacán, 04510 México D. F., Mexico

ARTICLE INFO

Article history:

Received 22 May 2014

Received in revised form

31 October 2014

Accepted 5 November 2014

Available online 2 December 2014

Keywords:

Thin liquid film

Thermocapillarity

Marangoni convection

Viscoelasticity

Thick wall

Codimension-two points

ABSTRACT

In this paper new results on linear viscoelastic thermal Marangoni convection are presented. The constitutive equation assumed is that of the Maxwell viscoelastic fluid. The competition between stationary and oscillatory convection is shown by means of plots of codimension-two points where the corresponding critical Marangoni numbers are the same. The variation of these points is investigated in a wide range of magnitudes of the thickness and thermal conductivity of the wall. Also, a discussion is given about the dependence they have on the Biot number of the fluid-atmosphere interface. Besides, it is shown how the range of the viscoelastic relaxation time corresponding to this points is modified by the Prandtl number.

© 2014 Elsevier Masson SAS. All rights reserved.

1. Introduction

Thin liquid films stability has important industrial applications. The problem of surface coating is one of them. The finishing of the coating is intimately related with the thermal Marangoni stability. The fractures found after solidification of the layer are strongly related with the Marangoni convection cells. The phenomenon has been investigated for Newtonian fluids since many years ago. Pearson [1] investigates the stationary stability of a thin layer with flat free surface considering different thermal boundary conditions. Scriven and Sternling [2] investigates for the first time the effect of free surface deformability. Takashima [3] considers the stationary free surface deformation of the layer and Takashima [4] includes the time dependence of the problem taking into account for the first time the effects of gravity in both papers. Mctaggart [5] studies the double diffusive problem of Marangoni convection when the free surface is flat. The Marangoni convection is investigated from a boundary layer point of view by Christopher and Wang [6]. Emphasis is put on the influence the Prandtl number has on heat transfer. Two free deformable surfaces can be present as in Ref. [7].

Convection in a layer with a free deformable surface and a deformable membrane is investigated in Ref. [8]. When the temperature gradient across the layer is large it is important to take into account the temperature variation of viscosity as in Slavtchev and Ouzounov [9] and Kalitzova-Kurteva et al. [10] for stationary convection with deformable free surface and in Slavtchev et al. [11] for oscillatory convection and deformable free surface. The control of Marangoni convection is important to avoid fractures in the solidification process as is investigated by Bau [12] and Or et al. [13]. In particular, Kechil and Hashim [14] assume free surface deformation and include viscosity dependence on temperature. An application to microchannels is presented in the paper by Pendse and Esmaeeli [15] who investigate the Marangoni flow in two superposed fluids when a spatially periodic temperature is applied to the wall. It is shown that the competition between thermal and hydrodynamic effects is reflected in the flow strength when the relative thickness of the layers is varied.

In applications the liquid usually presents a non Newtonian behavior. One important property is the viscoelasticity of the fluid (see Bird et al. [22]). In natural convection the viscoelastic linear and nonlinear effects have been investigated, for example, by Martínez-Mardones and colleagues [16–20]. In particular, in Ref. [17] one of the goals is to find the codimension-two point between stationary and oscillatory instability to investigate the

* Corresponding author.

E-mail address: ldavalos@unam.mx (L.A. Dávalos-Orozco).

Nomenclature

a	wave number
a_c	critical wave number
Bi_s	free surface-atmosphere Biot number
Bi_w	wall Biot number
d	d_w/d_f
d_f	fluid layer thickness
d_w	wall thickness
e	shear rate tensor
H_h	heat transfer coefficient
Ma	Marangoni number
Ma_c	critical Marangoni number
\vec{n}	free surface normal vector
P	pressure
p	pressure perturbation
Pr	Prandtl number
T	temperature
\bar{T}	liquid temperature
\bar{T}_w	wall temperature
T_h	temperature profile
u	perturbation velocity x-component

\vec{V}	fluid velocity vector
v	perturbation velocity y-component
w	perturbation velocity z-component

Greek

β	temperature gradient
Γ	surface tension
η	dynamic viscosity
θ	temperature perturbation
κ	fluid thermal diffusivity
κ_w	wall thermal diffusivity
λ	adimensional relaxation time (Weissenberg number)
λ_T	relaxation time
μ	viscoelastic parameter
ν	kinematic viscosity
ρ	fluid density
σ	oscillation frequency
τ	shear stress tensor
χ	χ_f/χ_w
χ_f	fluid thermal conductivity
χ_w	wall thermal conductivity

possibility of nonlinear traveling and stationary waves. For a review of this problem see Dávalos-Orozco [21].

Viscoelasticity have been taken into account in Marangoni convection by a number of authors. Getachew and Rosenblat [23] investigate the problem of a flat free surface assuming a very good conducting wall. Their main concern is to calculate the points where the curves of criticality of stationary convection intersect those of oscillatory viscoelastic convection. These intersections are called codimension-two points (see Ref. [17]). Wilson [24] investigates the instability growth rates of viscoelastic fluids with particular interest on slightly supercritical situations. Siddheshwar et al. [25], for temperature dependent viscosity, explore the oscillatory Marangoni instability of different non Newtonian fluids, in particular, the Maxwell fluid. They also assume a variety of thermal boundary conditions.

From the point of view of the linear equations, the stationary and oscillatory Marangoni convections differ not only by the absence of the time derivative in the stationary problem, but also by the presence of the Prandtl number in the oscillatory case. Physically, in stationary Marangoni convection the fluid particles are able to describe closed trajectories. This is due to the shear flow produced by the thermal perturbations which, from the wall, reach the free surface and modify the temperature dependent surface tension. If hot particles are continuously able to reach the free surface the cellular flow can be sustained heating from the wall. In oscillatory convection, all particles move at once in trajectories due to the shear flow produced by the weakening of surface tension. Nevertheless, they are not able to complete closed trajectories when the fluid has relatively high thermal diffusivity. In non dimensional form this is determined by the Prandtl number, that is, the ratio of the mass diffusivity (kinematic viscosity) over the heat diffusivity. Under these conditions, the fluid particle cools easily and it is not able to reinforce the shear flow by the weakening of surface tension. Consequently, the strong surface tension of the cold regions of the free surface dominate and the surface shear works in the opposite direction making all the particles in the bulk to go backwards to the wall where they are heated again to repeat the same process.

Therefore, depending on the Prandtl number the Marangoni convection may be stationary or oscillatory, as will be shown presently. However, it is well known that the linear Marangoni convection of a Newtonian fluid layer with a flat free surface only can be stationary (see Ref. [26]). If the free surface of a Newtonian fluid layer is allowed to deform, thermocapillary oscillations may appear first [2,4]. However, the case of a viscoelastic fluid layer with a flat free surface is different. The new degrees of freedom of the macromolecules added to the liquid motion by means of the constitutive equations, allow oscillatory Marangoni convection to appear for a smaller temperature gradient than that of the Newtonian fluid for some magnitudes of the Prandtl number and relaxation times [23].

The effect of a thick wall in Marangoni convection is investigated by Takashima [27]. The simultaneous effect of gravity and thermocapillarity is investigated by Yang [28] including a wall with finite thickness. A temperature dependent viscosity is assumed by Char and Chen [29] in a liquid layer on a thick slab. A deformable free surface is assumed by Abidin et al. [30] in the presence of buoyancy effects. The heat generation and properties of a thick wall are considered in thermocapillary convection by Arifin and Bachok [31]. The non uniformity of the basic temperature gradient may have important consequences on the instability. This is taken into account by Shivakumara et al. [32] including a thick slab. The deformability of the free surface is assumed in a layer on a thick wall by Gangadharaiah [33].

The results of thermocapillary convection including a thick slab are more realistic than those of an infinitely good conducting wall. This effect has also been investigated in natural convection of a Maxwell viscoelastic fluid by Pérez-Reyes and Dávalos-Orozco [34]. There it is shown that for certain magnitudes of the Prandtl number a codimension-two point is found where stationary and oscillatory convection compete to be the first unstable one for a range of values of the non dimensional relaxation time (Weissenberg number). An important difference between this paper and ref. [34] for natural convection is that here the results are only focused on the codimension-two points and not on the curves of criticality. However, the curves of criticality have

to be calculated to generate the curves of the codimension-two points.

The goal of the present paper is to calculate the codimension-two points that occur in the Marangoni convection of a Maxwell viscoelastic fluid layer coating a thick wall with finite thermal conductivity. The free surface is considered to be flat but susceptible to thermocapillary shear stresses. The Biot number at the free surface-atmosphere interface is also taken into account. The results of this research are important because in real situations the liquid layers lay on non ideal walls which have finite thickness and thermal conductivity. In particular, the investigations presented in the open literature on viscoelastic films assume from the onset that the wall is made of a very good or a very bad heat conducting material. As will be shown presently, differences in the thickness of the wall may also have important consequences on the critical parameters of the problem. In this aspect, the results presented below are new with respect to those published before. That is, careful calculations are done in a very wide range of magnitudes of the wall Biot number to show that the middle section of this range is very important and must be taken into account when the stability of the layer is the relevant goal in applications. If the stability of real coating problems is based on results of a very good conducting wall, it is possible that the wall finishing will be different from the expected one.

The paper is organized as follows. The equations of motion and boundary conditions are presented in the next section. The numerical results are given in Section 3. The last Section 4 are the conclusions.

2. Thermocapillary convection

The physical system under investigation consists of a thin layer of viscoelastic incompressible fluid of depth d_f and thermal conductivity χ_f coating a wall of thickness d_w and thermal conductivity χ_w , as seen in Fig. 1. Gravity has been neglected and the system is heated from the outer side of the wall and cooled at the flat free surface in contact with an inviscid atmosphere. Due to the temperature dependent surface tension, the free surface is susceptible to shear stresses leading to Marangoni convection.

An important difference of this system with respect to those with very good or very bad thermal conducting walls is the presence of the ratios of fluid to wall thermal conductivities χ and wall to fluid thicknesses d . They appear in the boundary conditions and are defined as $\chi = \chi_f/\chi_w$ and $d = d_w/d_f$, respectively.

The governing equations for Marangoni convection of a viscoelastic Maxwell fluid layer are the balance of momentum, heat diffusion and continuity equations:

$$\frac{d\vec{V}}{dt} = -\frac{1}{\rho}\nabla P + \nabla \cdot \tau \tag{1}$$

$$\frac{d\bar{T}}{dt} = \kappa \nabla^2 \bar{T} \tag{2}$$

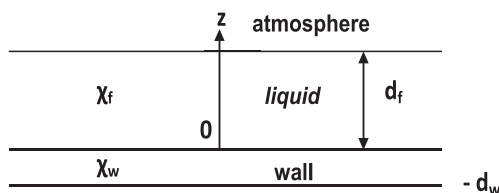


Fig. 1. Sketch of the system under research. A viscoelastic liquid layer coating a thick wall of thicknesses d_f and d_w , and thermal conductivities χ_f and χ_w , respectively.

$$\nabla \cdot \vec{V} = 0 \tag{3}$$

The temperature in the wall satisfies

$$\frac{\partial \bar{T}_w}{\partial t} = \kappa_w \nabla^2 \bar{T}_w \tag{4}$$

where $d/dt = \partial/\partial t + \vec{V} \cdot \nabla$. The shear stress tensor τ satisfies the constitutive equation for a Maxwell fluid model:

$$\tau + \lambda_T \frac{\mathcal{G}\tau}{\mathcal{G}t} = 2\eta \mathbf{e} \tag{5}$$

where \mathbf{e} is the shear rate tensor and $\mathcal{G}/\mathcal{G}t$ is a nonlinear operator which could be one of the upper convected, the lower convected or the corotational time derivatives, depending on the viscoelastic model selected. Note that when the hydrostatic state is perturbed, all the time derivatives of the linear equations are the same as the linear operator $\mathcal{G}/\mathcal{G}t = d/dt = \partial/\partial t$.

The boundary conditions are:

$$\vec{V} = 0 \quad \text{at } z = 0 \tag{6}$$

$$\tau \cdot \vec{n} = -\nabla \Gamma \quad \text{at } z = d_f \tag{7}$$

$$\bar{T}_w = T_0 + \Delta T \quad \text{at } z = -d_w \tag{8}$$

$$\bar{T} = \bar{T}_w \quad \text{and} \quad \chi \vec{n} \cdot \nabla \bar{T} = \vec{n} \cdot \nabla \bar{T}_w \quad \text{at } z = 0 \tag{9}$$

$$-\chi_f \vec{n} \cdot \nabla \bar{T} = H_h (\bar{T} - T_0) \quad \text{at } z = d_f \tag{10}$$

where \vec{n} is a normal vector which in the case of a flat free surface is in the z -direction and therefore $\vec{n} \cdot \nabla = \partial/\partial z$. H_h is the heat transfer coefficient. The gradient of the surface tension $\nabla \Gamma = (d\Gamma/dT)\nabla T$ depends on the temperature gradients and has projections on the x and y -directions. Notice that $d\Gamma/dT < 0$ in common fluids.

The nondimensional temperature profiles in hydrostatic conditions are:

$$T(z) = -z - \chi d \tag{11}$$

$$T_w(z) = -\chi z - \chi d \tag{12}$$

for the fluid and the wall, respectively. They were made adimensional subtracting $T_0 + \Delta T$ from the dimensional temperatures and then dividing by $\Delta T Bi_s / (1 + Bi_s + \chi d Bi_s)$. Here, the free surface-atmosphere Biot number is $Bi_s = H_h d_f / \chi_f$.

The main flow variables are perturbed from the hydrostatic state using $\vec{u} = (u(x, y, z, t), v(x, y, z, t), w(x, y, z, t))$, $p(x, y, z, t)$, $\theta(x, y, z, t)$, $\tau'(x, y, z, t)$, as the velocity, pressure, temperature and shear stress perturbations, respectively. The variables are made non dimensional using d_f for lengths, $\Delta T Bi_s / (1 + Bi_s + \chi d Bi_s)$ for temperature, v/d_f for velocity, d_f^2/κ for time and $\rho(\kappa/d_f)^2$ for pressure and shear stresses.

The non dimensional linearized equations for the perturbations are:

$$\frac{1}{Pr} \frac{\partial \vec{u}}{\partial t} = -\frac{\partial p}{\partial z} + \nabla \cdot \tau' \tag{13}$$

$$\frac{\partial \theta}{\partial t} - w = \nabla^2 \theta \tag{14}$$

$$\frac{\partial u}{\partial x} + \frac{\partial v}{\partial y} + \frac{\partial w}{\partial z} = 0 \tag{15}$$

where $Pr = \nu/\kappa$ is the Prandtl number. The perturbations of the shear stress tensor and shear rate tensor \mathbf{e}' satisfy:

$$\tau' + \lambda \frac{\partial \tau'}{\partial t} = 2\mathbf{e}' \tag{16}$$

Here, it is assumed that the perturbations are in the marginal state and that they have a normal modes representation in the form:

$$\{u, v, w, \theta\} = \{u'(z), v'(z), w'(z), \theta'(z), \theta'_w(z)\} \exp[i(kx + my + \sigma t)] \tag{17}$$

where k and m are wave numbers in the x and y directions, respectively, and σ is the frequency of oscillation. In the marginal state the growth rate is zero.

The operator $1 + \lambda \partial/\partial t$ is applied to the linear momentum equation to introduce \mathbf{e}' by means of the linear constitutive equation. Then, the rotational operator is applied twice. Finally, the normal modes are introduced in all the equations to obtain:

$$(D^2 - a^2 - i\sigma)\theta'(z) + w'(z) = 0 \tag{18}$$

$$(D^2 - a^2) \left(\mu(D^2 - a^2) - \frac{i\sigma}{Pr} \right) w'(z) = 0 \tag{19}$$

where $D = d/dz$ and $a = k^2 + m^2$ is the magnitude of the wave-number. The viscoelastic parameter for the Maxwell fluid is defined as $\mu = 1/(1 + i\sigma\lambda)$.

The thermal boundary conditions for the perturbation amplitudes are:

$$\theta'_w = 0 \quad \text{at } z = -d_w \tag{20}$$

$$\theta' = \theta'_w, \quad \chi D\theta' = D\theta'_w \quad \text{at } z = 0 \tag{21}$$

Notice that it is possible to reduce the two temperature boundary conditions at $z = 0$ into one condition. That is:

$$D\theta' - Bi_w\theta' = 0 \quad \text{at } z = 0 \tag{22}$$

where the Biot number which describes the heat transfer at the wall–fluid interface is defined by $Bi_w = q/\chi \tanh(qd)$, with $q = a^2 + i\sigma$. The other boundary conditions are

$$w' = Dw' = 0 \quad \text{at } z = 0 \tag{23}$$

$$w' = \mu D^2 w' + a^2 Ma \theta' = D\theta' + Bi_s \theta = 0 \quad \text{at } z = 1 \tag{24}$$

The Marangoni number is defined by

$$Ma = \left(\frac{(-\partial\Gamma/\partial T)d_f}{\rho\nu\kappa} \right) \left(\frac{\Delta T Bi_s}{1 + Bi_s + \chi d Bi_s} \right).$$

The solutions of the set of Eqs. (18) and (19) with the boundary conditions from Eqs. (20)–(24) form an eigenvalue problem for Ma which depends on all the other parameters of the problem in the general implicit form

$$F(Ma, a, \sigma, \lambda, \chi, d, Pr, Bi_s, Bi_w) = 0. \tag{25}$$

In fact, this is a solvability condition needed to have a solution different from the trivial one for the amplitudes of the perturbation normal modes.

3. Numerical results

The solution of Ma in Eq. (25) is obtained numerically with the Maple package. The Eq. (25) is complex due to the presence of the frequency of oscillation. The marginal Ma is calculated fixing all the parameters except a and σ . For a given a the roots of the complex Ma are obtained. Then, σ is varied until the imaginary part of the complex Ma is zero. In this way, the set (a, σ, Ma) becomes a point of the marginal curves. The critical Ma_c is calculated varying a , following the same procedure, until the minimum of Ma is obtained. The corresponding wavenumber and frequency are called critical and written as a_c and σ_c . The goal is to find the range of the Weissenberg number λ for which stationary and oscillatory convection will compete to be the first unstable one, that is, to find the codimension-two points of the instability. High precision numerical calculations were performed using more digits than those used by default. The default number of digits used by Maple is 10. Nevertheless, more precision is needed due to the large changes the marginal parameters have with a small variation of the Weissenberg number λ . Therefore, to avoid round-off errors, it was decided to increase the number of digits used by Maple. Tests were done first with 15 digits and then with 20 and 25 digits. It was found that 20 digits were good enough to avoid large oscillations in the numerical values of the critical parameters. However, the running time of the program increases considerably as a consequence.

Assuming that the Prandtl number is very near to that of water, two Prandtl numbers are used in the calculations $Pr = 2$ (water between 85 and 90 °C) and $Pr = 10$ (water between 5 and 10 °C). The free surface Biot number will have the magnitudes $Bi_s = 0, 0.1, 2, 5$. Two magnitudes of $d = 0.1$ and 100 will be used because no important differences are observed in the ranges $d < 0.1$ and $d > 100$.

The results are plotted in graphs of Ma_c , a_c and σ_c vs. χ . The magnitudes of χ are inside the range $10^{-10} \leq \chi \leq 10^{10}$, that is, from a very good conducting wall to a very bad conducting wall. The curves of codimension-two points are plotted in the ranges where the Ma_c of stationary and oscillatory Marangoni convection are the same. Thus, the corresponding curves of wavenumbers and frequencies of oscillation are determined. Of particular importance in this paper are the corresponding curves of the Weissenberg number λ vs. χ . This is because they show where the increase of λ makes oscillatory convection the first unstable one when crossing the codimension-two curves.

3.1. Stationary Marangoni convection

The critical curves of stationary Marangoni convection are obtained setting from the onset $\sigma = 0$. In this way the flow behavior is Newtonian because $\mu = 1$. The Prandtl number does not play a role here. The problem includes the effect of Bi_s , d and χ inside Bi_w , in contrast to the work of Pearson [1].

The critical curves are calculated fixing Bi_s and d . The results are presented in plots of Ma_c and a_c against χ as in Fig. 2. According to the definition (see above Eq. (23)), Bi_w decreases when χ increases. Therefore, the wall becomes a bad heat conductor when χ is large and a good heat conductor when χ is small. As seen in Fig. 2, for stationary Marangoni convection Ma_c decreases with χ . In both limits the magnitudes of Ma_c and a_c differ according to the magnitude of Bi_s . This is illustrated in Table 1. From the table it is clear that an increase of χ is destabilizing and that an increase of Bi_s is stabilizing. These magnitudes are important to determine the limits for the codimension-two points investigated in the following sections.

In Fig. 2 it is shown that the influence of d is only relevant in the middle range of χ . This difference is more important when $Bi_s \leq 2$.

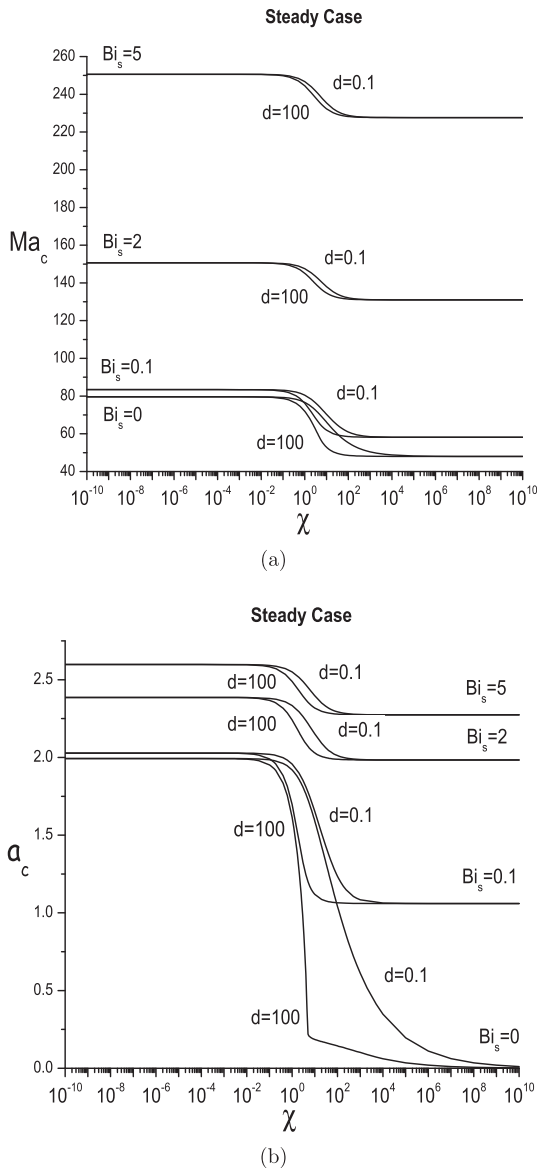


Fig. 2. Steady convection. Variation of a) the critical Marangoni number Ma_c and b) the critical wave number a_c with χ , for $Bi_s = 0, 0.1, 2, 5$ and thicknesses $d = 0.1$ and 100 .

There, Ma_c may show differences up to more or less 15 units (see Fig. 2a). Now, as seen in Fig. 2b, the influence of d on a_c is notable for $Bi_s \leq 2$. Clearly, a_c decreases with χ until it reaches its smallest magnitude in the limit $\chi \rightarrow \infty$. That limit is zero in the particular case of $Bi_s = 0$.

It is important to point out that the results shown in Fig. 2 are in agreement with those presented by Takashima [27]. Yet he only calculates curves for d up to $d = 10$. Those curves are inside the

Table 1
Limit magnitudes of stationary Ma_c and a_c .

Bi_s	$\chi \rightarrow 0$		$\chi \rightarrow \infty$		Differences	
	Ma_c	a_c	Ma_c	a_c	$Ma_{c0} - Ma_{c\infty}$	$a_{c0} - a_{c\infty}$
0	79.607	1.993	48	0	31.606	1.993
0.1	83.426	2.028	58.150	1.06	25.276	0.968
2	150.678	2.386	131.016	1.984	19.661	0.402
5	250.597	2.598	227.662	2.274	22.935	0.324

range of our calculations. Notice that the parameter he uses corresponds to the algebraic inverse of χ in this paper.

3.2. Oscillatory convection

Here it is of interest to calculate the Ma_c corresponding to viscoelastic oscillatory Marangoni convection. The magnitude of Ma_c depends on σ , Pr and λ and on those parameters of stationary convection. For given a , χ , Bi_s , Pr and λ , Ma is solved from Eq. (25) using Maple. The Marangoni number is complex $Ma = Ma_r + iMa_i$ due to the presence of σ , where Ma_r is the real part and Ma_i is the imaginary part. The Marangoni number should be real. Thus, it is necessary to calculate the root of $Ma_i = 0$ with respect σ . This root is the marginal σ which is substituted into Ma_r to obtain the marginal Marangoni number $Ma = Ma_r$. With all the other parameters fixed, a new a is given to calculate another marginal σ and Ma . This process is followed until a minimum is found of all the marginal Ma 's. This minimum is called the critical Marangoni number Ma_c with its corresponding critical wavenumber a_c and critical frequency of oscillation σ_c . The other parameters are varied to give all the curves of criticality. Sample curves are found in Fig. 3. Notice

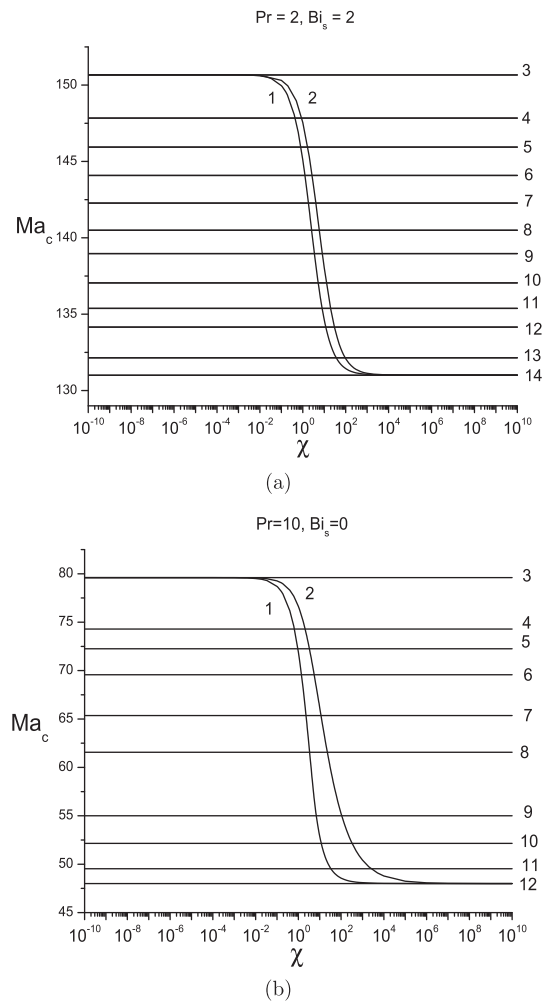


Fig. 3. Codimension-two points calculation with Ma_c vs χ plots. Two samples: 3a) $Pr = 2$ and $Bi_s = 2$. 1: stationary: $d = 100$, 2: stationary $d = 0.1$. Critical curves for the λ 's: 3: 0.0594, 4: 0.0606, 5: 0.0614, 6: 0.0622, 7: 0.063, 8: 0.0638, 9: 0.0645, 10: 0.0654, 11: 0.0662, 12: 0.0668, 13: 0.0678, 14: 0.0684. 3b) $Pr = 10$ and $Bi_s = 0.1$: stationary $d = 100$, 2: stationary $d = 0.1$. Critical curves for the λ 's: 3: 0.0548, 4: 0.0585, 5: 0.06, 6: 0.0622, 7: 0.0659, 8: 0.0696, 9: 0.0770, 10: 0.0807, 11: 0.0844, 12: 0.0867.

that for a fixed Bi_s , the curves of Ma_c vs χ are almost horizontal. That is, the calculated change is only around one hundredth in the range of χ used.

This small dependence of Ma_c of oscillatory convection on χ has the influence of the Prandtl number. Calculations for $Pr = 0.1$ and 0.5 have been done too in order to check the numerical results with those of Getachew and Rosenblat [23] and for the sake of comparison with the results of this paper. For $Pr = 0.5$, Ma_c has variations of a few decimals and for $Pr = 0.1$ it has variations of a few units. The a_c and σ_c of both cases only have variations of a few decimals. Therefore, it can be said that for $0.1 \leq Pr \leq 10$, the critical Ma_c , a_c and σ_c are almost constant in the range of χ investigated and that the wall geometry and thermal boundary conditions have no effect on the oscillatory instability. In this regard, for fixed Bi_s and Pr , the variation of Ma_c of the codimension-two points with respect to χ is due to the dependence on λ of the oscillatory Ma_c and to the dependence on χ of the stationary Ma_c .

Fig. 3a shows results for $Pr = 2$ and $Bi_s = 2$. The curves of criticality decrease with an increase of λ . Thus, λ has a destabilizing effect. In this example, oscillatory convection is the first unstable one in a range of χ starting from $\lambda > 0.0594$. Only oscillatory convection appears for $\lambda > 0.0684$. The example of Fig. 3b shows results for $Pr = 10$ and $Bi_s = 0$. When $\lambda > 0.0548$ oscillatory convection is the first unstable one in a range of χ . Oscillatory convection prevails for all χ when $\lambda > 0.0867$.

From the results of Fig. 3, it is clear the sensitivity of the convective instability to small variations of the Weissenberg number λ . From $\lambda = 0.0594$ to 0.0684 , Ma_c decreases from 150.67 to 131.01, as shown in Fig. 3a (see also Table 1).

It is important to point out that, to determine the codimension-two curves of the instability, a larger number of curves of criticality of oscillatory convection have to be calculated than those shown in Fig. 3a and b. The codimension-two curves are obtained approximating the points of intersection (that is, those corresponding to the same Ma_c) between the stationary and oscillatory curves of criticality for the two values of d , as will be shown in the following subsection.

3.3. Codimension-two points

The codimension-two points are presented first for the Weissenberg number λ against χ , which is of main importance in this paper. The Prandtl number is fixed as $Pr = 2$ in Fig. 4. Fig. 4a shows how λ for the codimension-two point increases with χ for all the magnitudes of Bi_s . In particular, that increase is more important for small Bi_s where notable separations exist between the curves of $d = 100$ and 0.1 .

The physical meaning of the curves in Fig. 4a is that for λ 's larger than those of the codimension-two curves, the first unstable viscoelastic thermocapillary convection is oscillatory. Therefore,

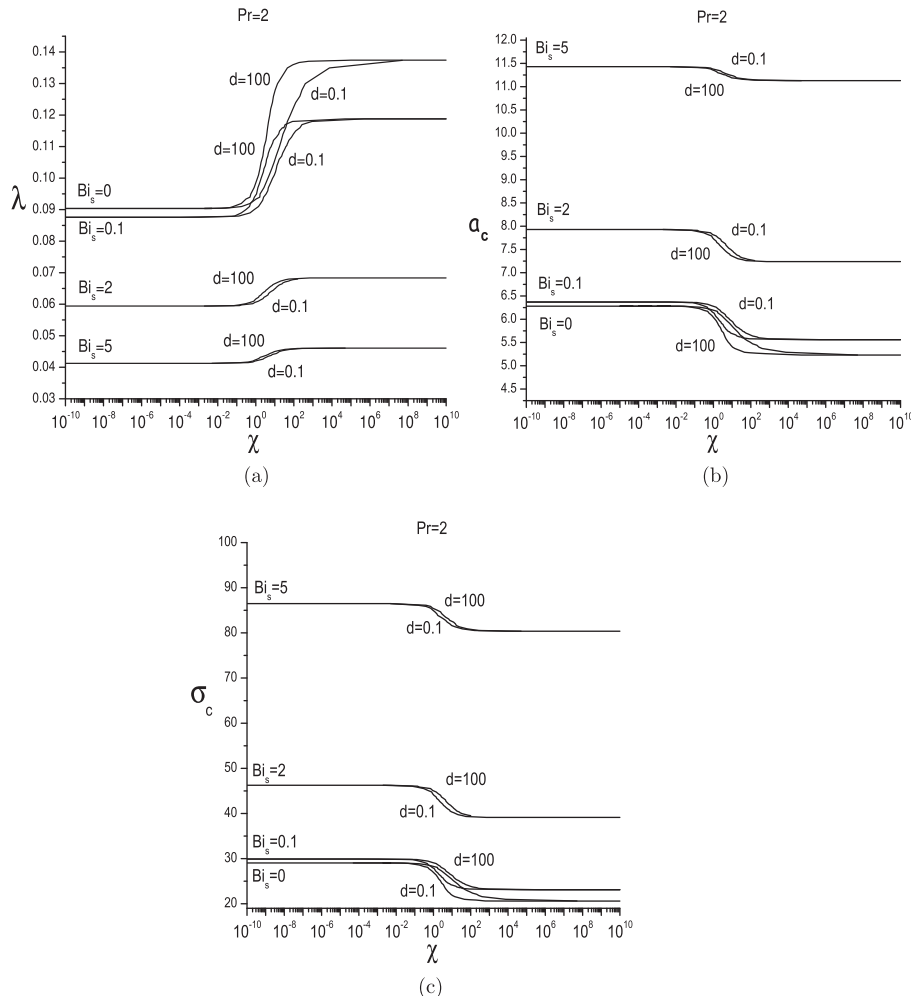


Fig. 4. Codimension-two points. λ , a_c and σ_c against χ , for $Pr = 2$ with $Bi_s = 0, 0.1, 2, 5$, and $d = 0.1$ and 100 . Notice that the magnitudes of a_c are different from those of the stationary case in Fig. 2b.

from the λ point of view, it is easier to have oscillatory convection for small χ .

In contrast, the curves of a_c of oscillatory convection in Fig. 4b of the codimension-two points, show a decrease with respect to χ . However, it is shown that in the case of oscillatory convection, a_c never tends to zero when $Bi_s \rightarrow 0$ and $\chi \rightarrow \infty$, as it occurs in stationary convection in Fig. 2b.

The frequency of oscillation at the codimension-two points follows a similar tendency as the wavenumber, that is, it decreases with χ . It is interesting to see that the frequency does not tend to zero when $Bi_s \rightarrow 0$ and $\chi \rightarrow \infty$. This is due to the finite wavenumber found in these two limits and to the important influence viscoelasticity has on thermocapillary convection.

The next Fig. 5 for $Pr = 10$ shows the relevant role played by the Prandtl number on the codimension-two points. In Fig. 5a it is shown how the magnitudes of λ decrease considerably. However, the behavior with respect to χ is similar to that of Fig. 4a. The curves of the wavenumber in Fig. 5b present a different reaction with respect to the change of Pr . With $Pr = 10$ their magnitudes increase more than hundred percent in some cases, mainly for small values of Bi_s . The behavior of the curves of a_c with respect to χ is similar to that of Fig. 4b. The corresponding frequencies of oscillation shown in Fig. 5c increase with $Pr = 10$ up to seven times the magnitudes of Fig. 4c for small Bi_s . However, their behavior with respect to χ is similar.

The results of Figs. 4 and 5 have been checked with the results of Getachew and Rosenblat [23] (see their Table 1). They correspond to $\chi = 10^{-10}$ and $Bi_s = 0$ of the figures. The case of $Pr = 2$ is corroborated by interpolation using a number of data of each column of their Table 1. Observe that the results of $Pr = 10$ correspond very well to those of [23]. Besides, the numerical algorithm was checked against all the data of their Table 1. To the authors best knowledge there is no paper published in the open literature with $Bi_s > 0$. It is important to point out that it is not possible to compare with the results of Siddheshwar et al. [25] because of the lack of numerical results for the Maxwell fluid and due to the very scarce numerical results for the Oldroyd model (for constant viscosity). They only calculate the case $Pr = 10$ for an Oldroyd fluid with a Weissenberg number equal to 0.3 and ratio of the retardation and relaxation times equal to 0.33 (very large and far from the Maxwell fluid model).

The results presented above can be seen in a different way. The Marangoni numbers of the codimension-two points are now plotted in Fig 6 against a_c , σ_c and λ . The plots are grouped into “columns” which are tagged with the corresponding characteristic of the flow and Prandtl number. If the flow is stationary the “column” is tagged with “st”. When the flow is oscillatory the “column” is tagged with the corresponding Prandtl number, that is, $Pr = 2$ or $Pr = 10$. Notice that only Fig. 6a has three plot “columns”. The

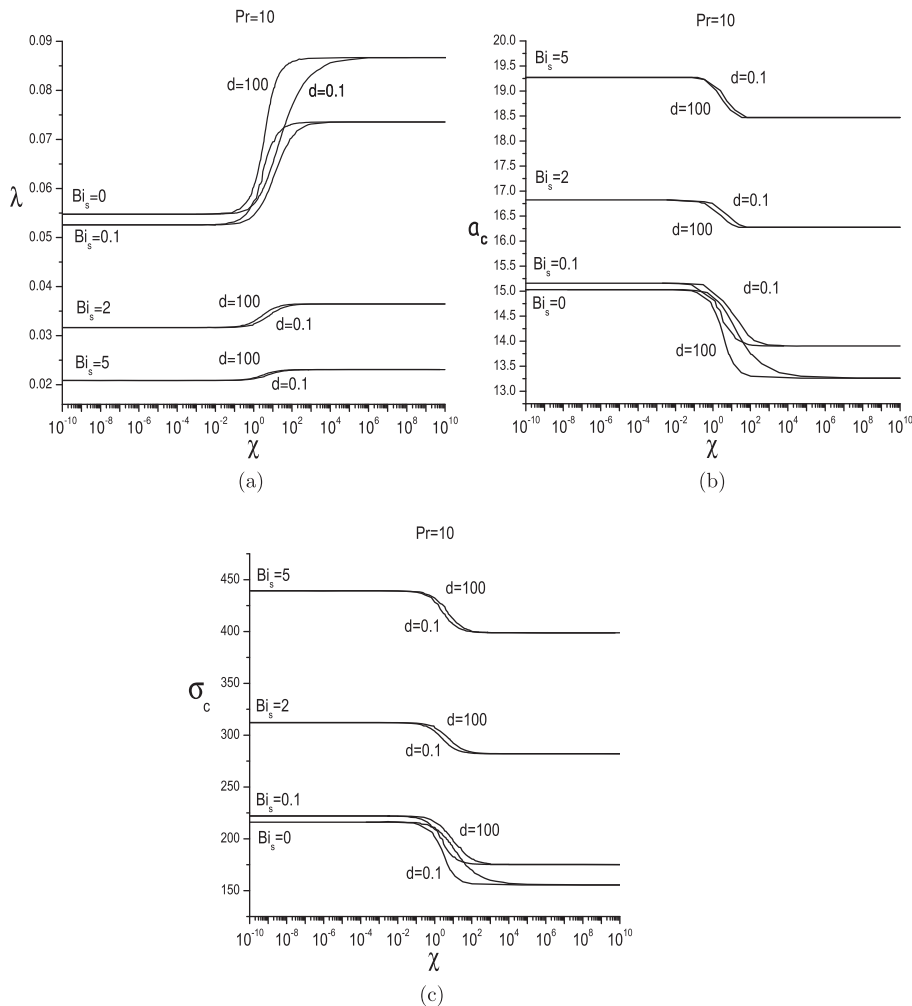


Fig. 5. Codimension-two points. λ , a_c and σ_c against χ , for $Pr = 10$ with $Bi_s = 0, 0.1, 2, 5$, and $d = 0.1$ and 100 . Notice that the magnitudes of a_c are different from those of the stationary case in Fig. 2b.

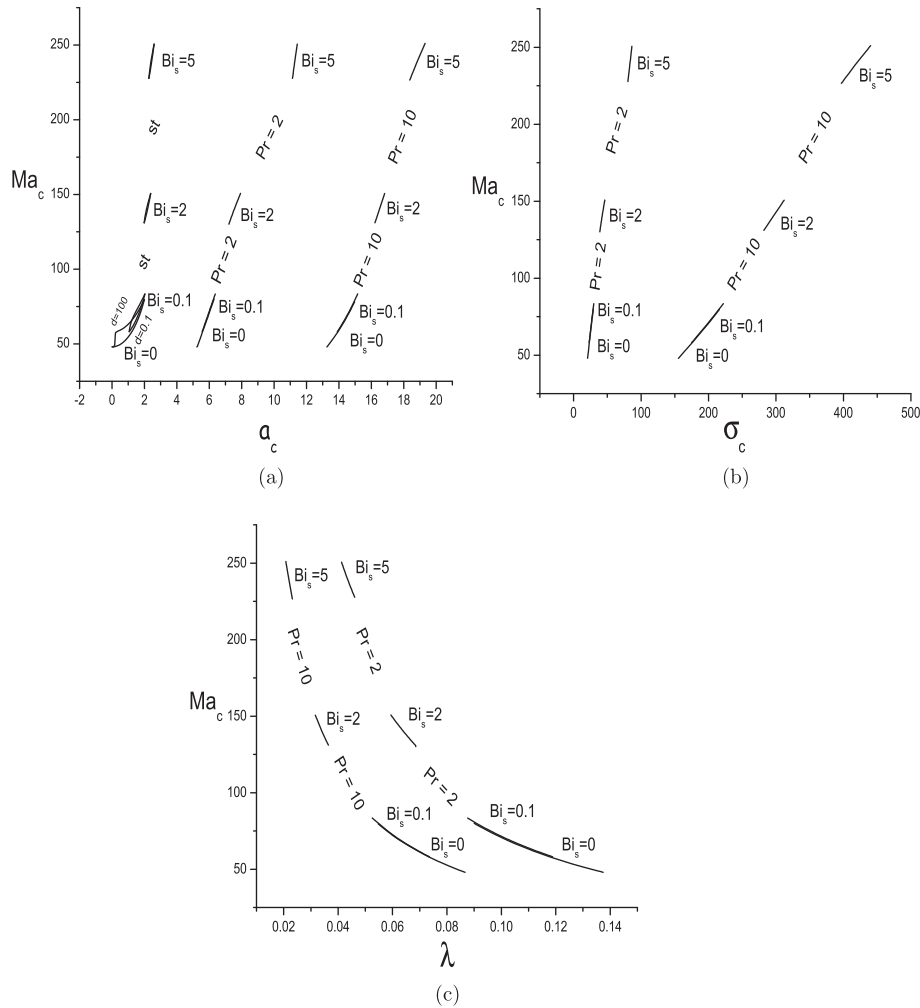


Fig. 6. Ma_c against a_c , σ_c and λ . For $Pr = 2, Pr = 10, Bi = 0, 0.1, 2, 5$ and $d = 0.1$ and 100 . When the tags are Pr the flow is oscillatory and when the tags are st the flow is stationary. 6a) Ma_c vs a_c , 6b) Ma_c vs σ_c and 6c) Ma_c vs λ .

reason is that it includes plots of the wavenumbers of stationary convection which, as explained above, are different from those of oscillatory convection. It is noteworthy that the separation of the curves due to $d = 0.1$ and 100 is only clear in the “column” of stationary convection (st) in Fig. 6a when Bi_s is 0 and 0.1. The reason is that the scale adopted to review the results is not wide enough to show the separation in the other plots.

In this way, Fig. 6 gives us a full panorama of the thermocapillary behavior of the Maxwell viscoelastic fluid. The parameters involved in the problem are shown as a map of its behavior. The magnitude of the parameters are shown just beside the corresponding curve.

Ma_c is plotted against a_c in Fig. 6a. By definition the range of Ma_c of the codimension-two points is the same as that of the stationary Ma_c for a fixed Bi_s and independent of Pr . Observe that the Marangoni numbers of the codimension-two points increase with Bi_s which therefore has a stabilizing effect. The corresponding magnitudes of the wavenumbers increase with Pr , as shown in the “columns” for $Pr = 2$ and $Pr = 10$.

The frequencies of oscillation in Fig. 6b increase too with Pr . However, when $Pr = 10$ the influence of Bi_s is stronger as seen by the large inclination of the “column”, where Ma_c and σ_c have a remarkable increase.

The “columns” of the codimension-two points in Fig. 6c are also inclined but in a different direction. This means that Ma_c of the codimension-two points decreases with an increase of λ . Thus, λ has

a destabilizing effect. It is clear that an increase of Bi_s stabilizes. Notice that for $Pr = 10$ smaller magnitudes of λ can destabilize the flow and that the curves of criticality can cross through the codimension-two points in a shorter range of λ .

3.4. Importance of d

The thicknesses ratio has important influence on the instability. This effect is transmitted to the codimension-two curves, as is apparent in the figures presented above. Yet it is not clear quantitatively how large is the separation between the two curves of $d = 0.1$ and 100 for each of the parameters under investigation such as a_c for stationary (st) convection, a_c for oscillatory convection, σ and λ . These parameters have different magnitudes for each Bi_s used in this paper. It is found that the largest separation of the curves of $d = 0.1$ and 100 is located not exactly but near to $\chi = 10$. Therefore, Table 2 is used to present the numerical calculation of the separation of the two curves at $\chi = 10$. Four magnitudes of the parameter $Bi_s = 0, 0.1, 2$ and 5 are used which correspond to each column in the table.

It is clear that the separation of the codimension-two curves, for each of the parameters, decreases with the increase of Bi_s . A slight increase is observed for $Bi_s = 5$ when $Pr = 10$, but it is important to remember that the differences found at $\chi = 10$ not necessarily are uniform. Observe that $Pr = 10$ imposes an extra effect on the

Table 2
Difference between $d = 0.1$ and 100 .

Effect at $\chi = 10$				
Bi_s	0	0.1	2	5
Ma_c st	13.276	8.386	3.398	3.068
a_c st	1.404	0.533	0.122	0.079
$Pr = 2$				
λ	0.02150	0.01143	0.00163	0.00068
a_c	0.424	0.265	0.114	0.038
σ_c	3.403	2.189	1.164	0.798
$Pr = 10$				
λ	0.01454	0.00767	0.00088	0.00031
a_c	0.789	0.445	0.104	0.114
σ_c	25.958	15.849	5.203	5.263

oscillatory case producing large differences of the frequencies of oscillation in comparison with $Pr = 2$.

From Table 2 it is possible to conclude that the increase of Bi_s improves the heat conducting properties at the surface-atmosphere boundary. Consequently, the thicknesses ratio becomes less relevant.

4. Conclusions

The codimension-two points of Marangoni convection in a Maxwell viscoelastic fluid layer have been investigated under the influence of a number of parameters. They are the Weissenberg number λ , the thicknesses ratio d , the heat conductivities ratio χ , the Prandtl number Pr and the fluid-atmosphere Biot number Bi_s . All of them have an important effect on the Marangoni instability.

It is found that λ has to grow to reach the codimension-two point when χ increases. Physically, this means that when the wall heat conductivity decreases in relation with that of the fluid, the fluid elasticity has to increase in order to allow oscillatory convection to compete to be the first unstable one. Further, when the relative wall thickness increases by means of d , λ has to increase even more. On the contrary, when the heat flux through the free surface Bi_s increases, the λ needed to reach the codimension-two point is smaller. Notice that the ranges of λ are reduced too and that Ma_c increases considerably stabilizing the system.

It is shown that the increase of heat conductivities ratio decreases the stationary Marangoni number. This makes the competition between stationary and oscillatory convection more difficult. Therefore, it is necessary to increase the Weissenberg number (more elastic fluid) to allow oscillatory convection to be the first unstable one.

It is demonstrated that this effect is modified by the Prandtl number. An increase of Pr (that is, a decrease of the heat diffusivity of the fluid) decreases the magnitude of λ but, on the contrary, it increases the magnitudes of the wavenumber and the frequency of oscillation corresponding to the codimension-two points.

The separation between the curves of $d = 0.1$ and 100 is important to show the relevance of this parameter on the stability. Geometrically, their meanings are that the thickness of the wall is 10 times smaller and 100 times larger than that of the fluid layer, respectively. Table 2 presents the separation of the curves, for fixed $\chi = 10$ and for different parameters taking into account that they depend on Bi_s . It is clear that the separations of λ and the other parameters of the problem decrease with an increase of Bi_s . Physically, the relative increase of heat flux across the free surface (Bi_s) makes ineffective the geometry of the thick wall reflected in the parameter d .

In comparison with previous papers on viscoelastic Marangoni convection, this work presents results more useful in realistic practical and laboratory conditions. The reason is that the

geometric and physical properties of the wall are taken into account. Notice that the use of the results of ideal wall thermal boundary conditions in applied coating problems may lead to unexpected results. Therefore, from the results of this paper, it is important to consider the relevance of the middle section of the range of χ to understand the stability and the codimension-two points expected in applications.

The next step is to calculate the codimension-two points of an Oldroyd fluid where an extra parameter appears. That is, the retardation time.

Acknowledgments

The authors would like to thank, Joaquín Morales, Cain González, Raúl Reyes, Alberto López, Ma. Teresa Vázquez and Oralía Jiménez for technical support.

References

- [1] J.R.A. Pearson, On convection cells induced by surface tension, *J. Fluid Mech.* 4 (1958) 489–500.
- [2] L.E. Scriven, C.V. Sternling, On cellular convection driven by surface-tension gradients: effects of mean surface tension and surface viscosity, *J. Fluid Mech.* 19 (1964) 321–340.
- [3] M. Takashima, Surface tension driven instability in a horizontal liquid layer with a deformable free surface. I. Stationary convection, *J. Phys. Soc. Jpn.* 50 (1981a) 2745–2750.
- [4] M. Takashima, Surface tension driven instability in a horizontal liquid layer with a deformable free surface. II. Overstability, *J. Phys. Soc. Jpn.* 50 (1981b) 2751–2756.
- [5] C.L. McTaggart, Convection driven by concentration and temperature dependent surface tension, *J. Fluid Mech.* 134 (1983) 301–310.
- [6] D.M. Christopher, B.-X. Wang, Prandtl number effects for Marangoni convection over a flat surface, *Int. J. Therm. Sci.* 40 (2001) 564–570.
- [7] L.A. Dávalos-Orozco, Thermocapillary instability of liquid sheets in motion, *Colloids Surfaces A* 157 (1999) 223–233.
- [8] L.A. Dávalos-Orozco, Thermal Marangoni convection of a fluid film coating a deformable membrane, *J. Colloid Interfaces Sci.* 234 (2001) 106–116.
- [9] S. Slavtchev, V. Ouzounov, Stationary Marangoni instability in a liquid layer with temperature-dependent viscosity in microgravity, *Microgravity Q.* 4 (1994) 33–38.
- [10] P.G. Kalitzova-Kurteva, S.G. Slavtchev, I.A. Kurtev, Stationary Marangoni instability in a liquid layer with temperature-dependent viscosity and deformable free surface, *Microgravity Sci. Technol.* 9 (1996) 257–263.
- [11] S.G. Slavtchev, P.G. Kalitzova-Kurteva, I.A. Kurtev, Oscillatory Marangoni instability in a liquid layer with temperature-dependent viscosity and deformable free surface, *Microgravity Sci. Technol.* 11 (1998) 29–34.
- [12] H.H. Bau, Control of Marangoni-Bénard convection, *Int. J. Heat. Mass Transf.* 42 (1999) 1327–1341.
- [13] A.C. Or R.E. Kelly, L. Cortezzi, J.L. Speyer, Control of long-wavelength Marangoni-Bénard convection, *J. Fluid Mech.* 387 (1999) 321–341.
- [14] S.A. Kechil, I. Hashim, Oscillatory Marangoni convection in variable viscosity fluid layer: the effect of thermal feedback control, *Int. J. Therm. Sci.* 48 (2009) 1102–1107.
- [15] B. Pendse, A. Esmaeeli, An analytical solution for thermocapillary-driven convection of superposed fluids at zero Reynolds and Marangoni numbers, *Int. J. Therm. Sci.* 49 (2010) 1147–1155.
- [16] J. Martínez-Mardones, C. Pérez-García, Linear instability in viscoelastic fluid convection, *J. Phys. Condens. Matter* 2 (1990) 1281–1290.
- [17] J. Martínez-Mardones, R. Tiemann, D. Walgraef, W. Zeller, Amplitude equations and pattern selection in viscoelastic convection, *Phys. Rev. E* 54 (1996) 1478–1488.
- [18] J. Martínez-Mardones, R. Tiemann, D. Walgraef, Convective and absolute instabilities in viscoelastic fluid convection, *Phys. A* 268 (1999) 14–23.
- [19] D. Laroze, J. Martínez-Mardones, L.M. Pérez, Amplitude equation for stationary convection in a viscoelastic magnetic fluid, *Int. J. Bifurcation Chaos* 20 (2010) 235–242.
- [20] D. Laroze, L.M. Pérez, J. Bragard, E.G. Cordaro, J. Martínez-Mardones, Magneto-hydrodynamics 47 (2011) 159–165.
- [21] L.A. Dávalos-Orozco, Viscoelastic natural convection, in: J. de Vicente (Ed.), *Viscoelasticity – from Theory to Biological Applications*, Intech, Rijeka, 2012, pp. 3–32 (Open access).
- [22] R.B. Bird, R.C. Armstrong, O. Hassager, *Dynamics of Polymeric Liquids Vol. 1: Fluid Mechanics*, second ed., Wiley-Interscience, New York, 1987.
- [23] D. Getachew, S. Rosenblat, Thermocapillary instability of a viscoelastic liquid layer, *Acta Mech.* 55 (1985) 137–149.
- [24] S.R.D. Wilson, Growth rates of the Marangoni instability in a layer of elastic fluid, *Rheol. Acta* 34 (1995) 601–605.

- [25] P.G. Siddheshwar, G.N. Sekhar, G. Jayalatha, Surface tension driven convection in viscoelastic liquids with thermorheological effect, *Int. Commun. Heat Mass Transf.* 38 (2011) 468–473.
- [26] A. Vidal, A. Acrivos, The nature of the neutral state in surface-tension driven convection, *Phys. Fluids* 9 (1966) 615–616.
- [27] M. Takashima, Surface-tension driven convection with boundary slab of finite conductivity, *J. Phys. Soc. Jpn.* 29 (1970), 531–531.
- [28] H.Q. Yang, Boundary effect on the Bénard-Marangoni instability, *Int. J. Heat. Mass Transf.* 35 (1992) 2413–2420.
- [29] M.-I. Char, C.-C. Chen, Influence of viscosity variation on the stationary Bénard-Marangoni instability with a boundary slab of finite conductivity, *Acta Mech.* 135 (1999) 181–198.
- [30] N.Z. Abidin, N.M. Arifin, M.S.M. Noorani, Boundary effect in Marangoni convection in a variable viscosity fluid layer, *J. Math. Stat.* 4 (2008) 1–8.
- [31] N.M. Arifin, N. Bachok, Boundary effect on the onset of Marangoni convection with internal heat generation, *World Acad. Sci., Eng. Tech* 38 (2008) 20–23.
- [32] I.S. Shivakumara, S.P. Suma, Y.H. Gangadharaiah, Effect of non-uniform basic temperature gradients on Marangoni convection with a boundary slab of finite conductivity, *Int. J. Eng. Sci. Tech.* 5 (2011) 4151–4160.
- [33] Y.H. Gangadharaiah, Onset of surface tension driven convection in a fluid layer with a boundary slab of finite conductivity and deformable free surface, *Int. J. Math. Arch.* 4 (2013) 311–323.
- [34] I. Pérez-Reyez, L.A. Dávalos-Orozco, Effect of thermal conductivity and thickness of the walls in the convection of a viscoelastic Maxwell fluid layer, *Int. J. Heat. Mass Transf.* 54 (2011) 5020–5029.